



Kinetic bottlenecks to respiratory exchange rates in the deep-sea – Part 1: Oxygen

A. F. Hofmann^{1,2}, E. T. Peltzer¹, and P. G. Brewer¹

¹Monterey Bay Aquarium Research Institute (MBARI), 7700 Sandholdt Road, Moss Landing, CA 95039-9644, USA

²German Aerospace Center (DLR), Institute of Technical Thermodynamics, Pfaffenwaldring 38–40, 70569 Stuttgart, Germany

Correspondence to: A. F. Hofmann (andreas.hofmann@dlr.de)

Received: 9 September 2012 – Published in Biogeosciences Discuss.: 11 October 2012

Revised: 14 June 2013 – Accepted: 25 June 2013 – Published: 25 July 2013

Abstract. Ocean warming is now reducing dissolved oxygen concentrations, which can pose challenges to marine life. Oxygen limits are traditionally reported simply as a static concentration threshold with no temperature, pressure or flow rate dependency. Here we treat the oceanic oxygen supply potential for heterotrophic consumption as a dynamic molecular exchange problem analogous to familiar gas exchange processes at the sea surface. A combination of the purely physico-chemical oceanic properties temperature, hydrostatic pressure, and oxygen concentration defines the ability of the ocean to provide the oxygen supply to the external surface of a respiratory membrane. This general oceanic oxygen supply potential is modulated by further properties such as the diffusive boundary layer thickness to define an upper limit to oxygen supply rates. While the true maximal oxygen uptake rate of any organism is limited by gas transport either across the respiratory interface of the organism itself or across the diffusive boundary layer around an organism, controlled by physico-chemical oceanic properties, it can never be larger than the latter. Here, we define and calculate quantities that describe this upper limit to oxygen uptake posed by physico-chemical properties around an organism and show examples of their oceanic profiles.

ical combination of these properties that best describes the external boundary condition for the rate at which O₂ can be transported across membrane surfaces. Here, we focus on the theoretical background for characterization, description, and mapping of the impacts of ocean deoxygenation from a gas exchange rate perspective.

The rate controls of diffusive processes are well understood and embodied in Fick's First Law. The solubility of the metabolically important gases is well known as a function of salinity and temperature (Weiss, 1970, 1974; Garcia and Gordon, 1992). From this and the observed distributions, partial pressures can be calculated. Likewise, the diffusion coefficients of the substances in question and their variation with temperature, as well as generally accepted formulations of the linkages between boundary layer thickness and fluid flow, are known. From these fundamental principles and observations, one can derive combined quantities which embody the essential chemical and physical principles in useful ways to illustrate and predict future changes in the ocean.

The quantities we define here are meant to be used in physico-chemical models of the ocean, for mapping the changing O₂ supply capacity of areas of interest such as for climate change assessments or for inter-regional comparisons to assist in ecosystem-based management decisions, as in the designation and knowledge of marine protected areas (e.g. Palumbi et al., 2009; Tallis et al., 2011).

1 Introduction

One of the challenges facing ocean science is the need to make a formal connection between the emerging changes in the physico-chemical properties of the ocean, such as rising temperature and CO₂ levels and declining O₂, and the phys-

2 Oceanic oxygen supply: physico-chemical vs. organism-specific quantities

The O₂ demands of marine organisms have classically been described as a rate problem (e.g. Hughes, 1966) in which diffusive transport across a boundary layer driven by partial pressure differences takes place. As with gas exchange rates at the sea surface (e.g. Wanninkhof, 1992) where wind speed is a critical variable, bulk fluid flow velocity over the animal surface is important. An oxygen concentration value alone does not adequately describe this process. For example, giving only an oxygen concentration as a limit for oxygen supply specifies no temperature-dependent information, so that the same value is assumed to be limiting over a temperature span of possibly 30 °C. This can be overcome to some extent by providing pO_2 as a limiting value (Hofmann et al., 2011), but the rate problem for gas transfer across a diffusive boundary layer contains also terms for diffusivity, and the relationship between boundary layer thickness and velocity over the surface, and thus a much more complete description would be useful.

The challenge in defining generic properties that describe the ocean in a way that is relevant to generic membrane transport of O₂ is to separate as best as possible the purely physical terms which are universally applicable, such as temperature T , oxygen concentration [O₂], hydrostatic pressure P (together resulting in an oxygen partial pressure pO_2), diffusivity (resulting from salinity S , T , and P), and the basic fluid dynamical form of the dependence of boundary thickness on flow.

There is no debate over the T , [O₂], P , and diffusivity terms since these are fundamental, organism-independent ocean chemical properties. The difficulty is in providing a way of including the flow term as a generic, organism-independent principle. There is no doubt of the existence of a diffusive boundary layer that is present over all ocean surfaces, thus also over all respiratory gas exchange interfaces. Generic and simplified descriptions of boundary layers are essential and widely used also for air–sea gas exchange rates, mineral dissolution rates, and phytoplankton nutrient uptake rates. The most widely used formulation is based on the dimensionless Schmidt number (e.g. Santschi et al., 1991; Wanninkhof, 1992). This relationship is standard within the ocean sciences and physiology (e.g. Pinder and Feder, 1990) and is also used here based on a planar surface model for the molecular exchange surface, which works well for all but microscopic scales (Zeebe and Wolf-Gladrow, 2001). We derive all gas flux properties on a per-square-centimeter scale so as to provide a way to normalize for different respiratory surface areas.

We stress that the end result desired is to provide improved functions and profiles that better allow comparison between different ocean regions undergoing change in their oxygen supply potential as the ocean warms and O₂ levels decline.

3 Materials and methods

A list of symbols and abbreviations used throughout this paper can be found in Table 1.

3.1 The oceanic oxygen supply potential SP_{O_2}

Here we define the oceanic oxygen supply potential as the combination of pO_2 and diffusivity under in situ conditions constituting a theoretical maximal upper limit for respiratory O₂ uptake as provided by a given oceanic region.

Respiratory gas molecules expelled or taken up have to traverse both the respiratory interface and the diffusive boundary layer (DBL) in the medium surrounding the respiratory interface on the outside, i.e. the surrounding ocean. In general, either one of these steps can be the rate-limiting step for respiratory gas transport (see also the companion paper: Hofmann et al., 2013).

We denote E_{DBL} as the maximal diffusive oxygen flux if only the diffusive boundary layer would need to be traversed (hypothetically assuming insignificant respiratory interface barrier). And E_{int} as the maximal diffusive oxygen flux if only the respiratory interface would need to be traversed (hypothetically assuming insignificant boundary layer barrier). We can then write for the true total diffusive flux of oxygen E (in $\mu\text{mol O}_2 \text{ s}^{-1} \text{ cm}^{-2}$) into an animal across both barriers

$$E \leq \min(E_{int}, E_{DBL}), \quad (1)$$

which means the diffusive flux across both barriers E is always smaller than or equal to the maximal flux that the DBL transversion permits (i.e. E_{DBL}), and we can write

$$E \leq E_{DBL}. \quad (2)$$

E_{DBL} , however, can be expressed by the standard representation (e.g. Santschi et al., 1991; Boudreau, 1996; Zeebe and Wolf-Gladrow, 2001) of Fick's First Law, using gas partial pressures (e.g. Piiper, 1982; Feder and Burggren, 1985; Pinder and Burggren, 1986; Pinder and Feder, 1990; Maxime et al., 1990; Pelster and Burggren, 1996) as¹

$$E_{DBL} = \frac{D \rho_{SW}}{L K O'} \Delta pO_2|_{DBL}. \quad (4)$$

¹where ρ_{SW} is the in situ density of seawater (calculated according to Millero and Poisson (1981) as implemented in Hofmann et al. (2010)) in kg cm^{-3} ; D is the molecular diffusion coefficient for O₂ in $\text{cm}^2 \text{ s}^{-1}$, calculated from temperature and salinity, e.g. as given in Boudreau (1996, Chapter 4); L is the DBL thickness in cm; $\Delta pO_2|_{DBL}$ in μatm is the oxygen partial pressure difference across the DBL; and where $K O'$ is the apparent Henry's constant for O₂ in $\text{mol kg}^{-1} \text{ atm}^{-1}$ ($= \mu\text{mol kg}^{-1} \mu\text{atm}^{-1}$) at in situ conditions:

$$K O' = \frac{[O_2]}{pO_2([O_2], T, S, P)}, \quad (3)$$

where [O₂] in mol kg^{-1} here is the O₂ concentration and in the denominator $pO_2([O_2], T, S, P)$ in atm is the associated partial pressure of O₂ as a function of O₂ concentration, temperature, salinity

Table 1. List of symbols and abbreviations – listed in the order of their appearance in the manuscript.

Symbol	Unit	Meaning
[O ₂]	μmol kg ⁻¹	oxygen concentration
<i>p</i> O ₂	μatm	oxygen partial pressure
<i>S</i>		salinity
<i>T</i>	K or °C	bulk oceanic temperature
<i>P</i>	bar	(hydrostatic) pressure
DBL		diffusive boundary layer around the gas exchange interfaces
<i>E</i> _{DBL}	μmol s ⁻¹ cm ⁻²	<i>hypothetical</i> diffusion-only oxygen uptake rate per area of gas exchange interface <i>if only the DBL was to cross, hypothetically assuming no respiratory interface barrier</i>
<i>E</i> _{int}	μmol s ⁻¹ cm ⁻²	<i>hypothetical</i> diffusion-only oxygen uptake rate per area of gas exchange interface <i>if only the respiratory interface was to cross, hypothetically assuming no DBL over the exchange surface</i>
<i>E</i>	μmol s ⁻¹ cm ⁻²	true oxygen uptake rate per area of gas exchange interface across the DBL and the respiratory interface together
<i>D</i>	cm ² s ⁻¹	molecular diffusion coefficient for O ₂
ρ _{SW}	kg cm ⁻³	in situ density of seawater
<i>L</i>	cm	DBL thickness
<i>K</i> ′	mol kg ⁻¹ atm ⁻¹ (μmol kg ⁻¹ μatm ⁻¹)	apparent Henry's constant for O ₂
<i>K</i> ′ _{IS}	mol kg ⁻¹ atm ⁻¹	apparent Henry's constant for O ₂ at in situ conditions
<i>K</i> ′ _E	mol kg ⁻¹ atm ⁻¹	apparent Henry's constant for O ₂ at experimental conditions
<i>p</i> O ₂ ([O ₂], <i>T</i> , <i>S</i> , <i>P</i>)	atm	in situ oceanic oxygen partial pressure as a function of carbon dioxide concentration, temperature, salinity, and hydrostatic pressure
Δ <i>p</i> O ₂ _{DBL}	μatm	O ₂ partial pressure difference across the DBL
<i>p</i> O ₂ _f	μatm	ambient free stream oxygen partial pressure (outside of the DBL)
<i>p</i> O ₂ _s	μatm	oxygen partial pressure directly at the respiratory surface (outside of the organism, but past the DBL)
<i>SP</i> O ₂	μmol s ⁻¹ cm ⁻¹	oceanic O ₂ supply potential (see text for explanations)
<i>K</i>	cm s ⁻¹	mass transfer coefficient for O ₂
<i>u</i> ₁₀₀	cm s ⁻¹	free stream fluid flow velocity over gas exchange surfaces
<i>E</i> _{max}	μmol s ⁻¹ cm ⁻²	Maximal hypothetical oxygen uptake rate per area of gas exchange interface, as permitted by DBL diffusion limitation
<i>p</i> _f	μatm	minimal <i>p</i> O ₂ _f that is able to support a given <i>E</i> (all other conditions remaining constant)
<i>C</i> _f	μmol kg ⁻¹	minimal oxygen concentration [O ₂] that is able to support a given <i>E</i> (all other conditions remaining constant)

Combining Eqs. (2) and (4) results in

$$E \leq \frac{D \rho_{\text{SW}}}{L K'} \Delta p_{\text{O}_2}|_{\text{DBL}}. \quad (5)$$

With this inequality, we can calculate an upper boundary for the diffusive flux of O₂ into an animal, as posed by the barrier of the diffusive boundary layer and the local *p*O₂ in the oceanic environment surrounding it. The true oxygen flux into an animal might be limited by respiratory interface trans-

and hydrostatic pressure, first calculated conventionally from the oxygen saturation concentration (Garcia and Gordon, 1992) using potential temperature (*θ*; Bryden, 1973; Fofonoff, 1977). Resulting *p*O₂ values are then corrected for hydrostatic pressure (calculated from given depth values according to Fofonoff and Millard (1983)) according to Enns et al. (1965).

port², but it is always lower than the upper boundary defined by the right-hand side of Eq. (5).

The oxygen partial pressure difference across the DBL *p*O₂|_{DBL} can be expressed as

$$\Delta p_{\text{O}_2}|_{\text{DBL}} = p_{\text{O}_2}|_{\text{f}} - p_{\text{O}_2}|_{\text{s}}, \quad (6)$$

with *p*O₂|_f expressing the oxygen partial pressure in the free stream beyond the DBL and *p*O₂|_s expressing the oxygen partial pressure directly on the gas exchange surface of the organism. Since, obviously, *p*O₂|_s ≥ 0 atm, the following inequality always holds true:

$$\Delta p_{\text{O}_2}|_{\text{DBL}} \leq p_{\text{O}_2}|_{\text{f}}. \quad (7)$$

²Interface transport limitation is an important and interesting field of research; however, it is out of the scope and intention of the paper presented here.

Since our aim is to calculate an upper boundary for oxygen flux into an organism, we can simplify Eq. (5) by combining it with Eq. (7) to

$$E \leq \frac{D \rho_{\text{SW}} K O'}{L} p\text{O}_2|_{\text{f}}. \quad (8)$$

Equation (8) expresses the fact that the true respiratory gas exchange per unit area of gas exchange surface is always smaller than $\frac{D \rho_{\text{SW}} K O'}{L} p\text{O}_2|_{\text{f}}$. This expression, however, contains the DBL thickness L , which is an organism-specific quantity as it depends on the unique surface microstructure of the respiratory surface area and any unique characteristics of the organism shape and mode of swimming or pumping. So, in order to arrive at a purely physico-chemical quantity that describes the organism-independent oceanic propensity for supplying oxygen, we multiply Eq. (8) by L and arrive at

$$E L \leq D \rho_{\text{SW}} K O' p\text{O}_2|_{\text{f}}. \quad (9)$$

This allows us to define the oceanic oxygen supply potential SP_{O_2} in $\mu\text{mol s}^{-1} \text{cm}^{-1}$ as the upper limit (i.e. maximal value) for the product of the respiratory oxygen uptake rate E and the DBL thickness L .

$$SP_{\text{O}_2} := D \rho_{\text{SW}} K O' p\text{O}_2|_{\text{f}} = D \rho_{\text{SW}} [\text{O}_2]_{\text{f}} \quad (10)$$

Thus, SP_{O_2} is a purely physical oceanic property, not dependent on any organism-specific properties or characteristics. It can be used to generate profiles and maps that illuminate which regions of the ocean are better able to support aerobic marine life than can simple O_2 concentration profiles or maps, since it incorporates the essential T , P and further diffusion-related terms.

3.2 The generic maximal theoretical oxygen supply rate E_{max}

All respiratory external surfaces will have a diffusive boundary layer that provides the contact with the ocean waters, and the thickness of this will in the macroscopic case³ depend upon the external flow over this surface, whether passive or controlled by organism motions. The most generic case is a simple planar surface description of the flow dependency of L , as was used to describe the mineral dissolution experiments in Santschi et al. (1991): the DBL thickness L can be expressed as the fraction of the molecular diffusion coefficient D and the mass transfer coefficient K , which is a function of the fluid flow u_{100} .

$$L = \frac{D}{K(u_{100})}, \quad (11)$$

³In microscopic organisms, L is usually taken to be equal to the radius of the sphere of the microorganism (cf. e.g. Stolper et al., 2010) – in this case, our formulation for E_{max} can still be used with the appropriate L .

which effectively makes L a function of flow velocity u_{100} . Table 2 details this generic description of L as a function of u_{100} .

For a given free stream oxygen partial pressure $p\text{O}_2|_{\text{f}}$, substituting Eq. (11) into Eq. (8) allows us to define an upper limit or for the oxygen uptake rate E per unit area of respiratory interface supported by the given $p\text{O}_2|_{\text{f}}$ as

$$E_{\text{max}} := \frac{SP_{\text{O}_2}}{L} = \frac{D \rho_{\text{SW}} K O'}{L} p\text{O}_2|_{\text{f}}. \quad (12)$$

This definition of E_{max} as an upper limit for the oxygen uptake rate utilizes a simplified and generic model to describe L . E_{max} values are thus not biologically specific, but are intended solely to compare various oceanic regions in their *potential* to supply oxygen under given in situ conditions and to offer a rough estimate as to how flow rates over respiratory interfaces influence this potential.

3.3 The minimal oxygen concentration C_{f} supporting a given laboratory-determined E

The traditional use of only the oxygen concentration $[\text{O}_2]$ as a measure does not take into account the large regional variations in T , P , and further diffusion-related quantities, so it is useful to compare functions containing these properties with $[\text{O}_2]$ alone.

In order to explicitly describe and reveal the influence of temperature and diffusion while comparing various oceanic regions, warm and shallow, as well as deep and cold, to one another, we define another quantity in which we remove the effect of the oxygen content of the water. To explicitly include the important dependence of gas exchange on partial pressure (e.g. Piiper, 1982; Pinder and Feder, 1990; Pelster and Burggren, 1996; Childress and Seibel, 1998; Seibel et al., 1999) and the dependency of partial pressure on hydrostatic pressure (Enns et al., 1965), we assume a given oxygen uptake rate E (in $\mu\text{mol s}^{-1} \text{cm}^{-2}$ – without loss of generality we assume throughout the paper a generic value of $E = 20 \times 10^{-7} \mu\text{mol s}^{-1} \text{cm}^{-2}$), experimentally determined at diffusivities D and DBL thicknesses L equal to the respective in situ values, but at one atmosphere. From Eq. (8) we can then determine a relation between the free stream oxygen partial pressure $p\text{O}_2|_{\text{f}}$ and this given oxygen uptake rate E as

$$p\text{O}_2|_{\text{f}} \geq \frac{L}{D \rho_{\text{SW}} K O'_E} E, \quad (13)$$

which shows that $p\text{O}_2|_{\text{f}}$ has to be greater or equal to the right-hand side of Eq. (13) to support the given E . Again describing a limiting condition, we define p_{f} as the minimal $p\text{O}_2|_{\text{f}}$ that can support E as

$$p_{\text{f}} := \frac{L}{D \rho_{\text{SW}} K O'_E} E. \quad (14)$$

Table 2. Expressing the DBL thickness L as a function of water flow velocity: a generic planar surface description.

The DBL thickness L can be expressed as the fraction of the temperature-dependent molecular diffusion coefficient D for O_2 in $\text{cm}^2 \text{s}^{-1}$, calculated from temperature and salinity as given in Boudreau (1996, Chapter 4) using the implementation in the R package *marelac* (Soetaert et al., 2010), and the mass transfer coefficient K (Santschi et al., 1991; Boudreau, 1996):

$$L = \frac{D}{K}.$$

K can be calculated for O_2 from the water-flow-induced shear velocity u' in cm s^{-1} and the dimensionless Schmidt number Sc for O_2 (as calculated by linearly interpolating two temperature-dependent formulations for $S = 35$ and $S = 0$ in Wanninkhof (1992) with respect to given salinity):

$$K = a u' Sc^{-b},$$

with parameters a and b : Santschi et al. (1991): $a = 0.078$, $b = \frac{2}{3}$; Shaw and Hanratty (1977) (also given in Boudreau (1996)): $a = 0.0889$, $b = 0.704$; Pinczewski and Sideman (1974) as given in Boudreau (1996): $a = 0.0671$, $b = \frac{2}{3}$; Wood and Petty (1983) as given in Boudreau (1996): $a = 0.0967$, $b = \frac{7}{10}$. Due to small differences we use averaged results of all formulations.

u' can be calculated from the ambient current velocity at 100 cm away from the exchange surface u_{100} and the dimensionless drag coefficient c_{100} (Sternberg, 1968; Santschi et al., 1991; Biron et al., 2004):

$$u' = u_{100} \sqrt{c_{100}}.$$

c_{100} is calculated from the water flow velocity u_{100} as (Hickey et al., 1986; Santschi et al., 1991)

$$c_{100} = 10^{-3} \left(2.33 - 0.0526 |u_{100}| + 0.000365 |u_{100}|^2 \right).$$

As mentioned above, in order to compare with standard conditions at one atmosphere, we assume laboratory experimental conditions at one atmosphere, so the apparent Henry's Law constant KO'_E in Eqs. (13) and (14) is calculated with one atmosphere. To explicitly include the hydrostatic pressure dependency of partial pressure, i.e. to obtain the oxygen concentration that would result in p_f at in situ hydrostatic pressures, we have to convert p_f to a concentration using an apparent Henry's Law constant KO'_{IS} calculated at in situ hydrostatic pressure. Thus, we can define C_f , the minimum oxygen concentration $[O_2]$ in $\mu\text{mol kg}^{-1}$ the free flowing stream must have to sustain E , as

$$C_f := p_f KO'_{IS} = \frac{L}{D \rho_{SW}} \frac{KO'_{IS}}{KO'_E} E. \quad (15)$$

The inclusion of the ratio of the Henry's Law constants at one atmosphere and at in situ pressures explicitly includes the pressure dependency of partial pressures, which makes C_f a quantity that can be used to directly compare warm and shallow to cold and deep oceanic regions.

3.4 Example oceanographic data

All T , S , P , and $[O_2]$ data for ocean profiles have been extracted from the Ocean Data View (Schlitzer, 2010) version of the World Ocean Atlas 2009 oxygen climatology (Garcia et al., 2010). Calculations have been performed in the

open-source programming language R (R Development Core Team, 2010).

4 Results and discussion

As noted above, warming of the ocean (Levitus et al., 2005; Lyman et al., 2010) is reducing the oxygen concentration via the solubility effect, decreasing ventilation due to increased stratification and increasing oxygen drawdown from microbial mineralization of organic matter. Thus global ocean oxygen concentrations are declining (Chen et al., 1999; Jenkins, 2008; Stramma et al., 2008; Helm et al., 2011), and the combined effects of T and O_2 have an impact on aerobic performance (e.g. Poertner and Knust, 2007). Yet at the same time, increased temperature enhances diffusion and results in increased gas partial pressures for the same concentrations, both of which enhance diffusive oxygen uptake rates. The properties we define above allow for a comparison of the relative roles and impacts of these opposing changes in oceanic properties.

To illustrate our newly defined quantities, we have chosen a set of example stations from different ocean basins for comparative purposes. Table 3 provides a tabulation for the classical oxygen concentration ($[O_2]$) hydrographic depth profiles as well as depth profiles of all quantities defined in this paper, calculated with data from the World Ocean Atlas 2009 (Garcia et al., 2010) oxygen climatology for six

Table 3. Depth profiles of $[O_2]$, SP_{O_2} , E_{\max} , and C_f for example stations around the world. Details on the tabulated quantities can be found in the text. The units used are as follows: $[O_2]$: $\mu\text{mol kg}^{-1}$; SP_{O_2} : $10^{-7}\mu\text{mol kg}^{-1}\text{s}^{-1}\text{cm}^{-1}$; E_{\max} : $10^{-7}\mu\text{mol kg}^{-1}\text{s}^{-1}\text{cm}^{-2}$; C_f : $\mu\text{mol kg}^{-1}$. For all locations we assume a constant flow velocity of $u_{100}=2\text{cm s}^{-1}$; more realistic flow profiles or organism-specific descriptions of the DBL thickness L can be employed here. For C_f calculations we assume a generic constant value of $E = 20 \times 10^{-7}\mu\text{mol s}^{-1}\text{cm}^{-2}$. $T_E=5^\circ\text{C}$ and $S_E = 34$. NA indicates that values are not available for the respective depth. SC: Southern California (120.5°W , 29.5°N); WP: Western Pacific (126.5°E , 11.5°N); CH: Chile (75.5°W , 33.5°S); WA: Western Africa (6.5°E , 15.5°S); BB: Bay of Bengal (87.5°E , 18.5°N); MD: Mediterranean (18.5°E , 35.5°N).

depth	SC				WP				CH			
	$[O_2]$	SP_{O_2}	E_{\max}	C_f	$[O_2]$	SP_{O_2}	E_{\max}	C_f	$[O_2]$	SP_{O_2}	E_{\max}	C_f
0	239	46	221	16.72	225	46	227	14.73	196	48	262	9.76
50	246	46	218	17.80	235	44	211	17.46	200	49	264	9.88
100	230	40	183	20.75	226	41	192	18.81	198	46	245	10.73
200	143	22	96	26.41	211	37	176	19.14	176	33	161	16.66
300	85	13	54	28.57	202	36	167	19.20	135	22	98	23.22
400	44	6	26	30.17	199	35	162	19.20	91	14	58	27.35
500	23	3	13	31.27	193	34	157	19.15	78	11	47	29.65
600	16	2	9	32.06	188	33	152	19.05	90	13	52	30.65
700	15	2	9	32.62	187	33	151	18.90	96	14	55	31.46
800	18	3	10	33.07	184	32	148	18.72	94	13	53	31.92
900	22	3	12	33.35	185	32	148	18.53	92	13	50	32.50
1000	28	4	15	33.63	185	32	148	18.33	94	13	51	32.79
1100	32	4	17	33.81	186	32	149	18.11	96	13	51	33.18
1200	36	5	19	33.90	190	33	152	17.88	94	13	50	33.38
1300	41	6	21	33.95	185	32	148	17.66	101	14	52	33.61
1400	46	6	24	33.97	190	33	152	17.44	102	14	52	33.76
1500	53	7	27	33.93	181	31	144	17.20	108	14	55	33.73
2000	82	11	40	33.37	192	33	153	16.11	115	15	57	33.02
3000	118	15	56	29.99	183	32	147	14.06	142	18	68	30.11
4000	132	17	63	26.22	190	33	152	12.29	152	20	72	26.27

depth	WA				BB				MD			
	$[O_2]$	SP_{O_2}	E_{\max}	C_f	$[O_2]$	SP_{O_2}	E_{\max}	C_f	$[O_2]$	SP_{O_2}	E_{\max}	C_f
0	245	45	214	18.29	222	46	233	13.88	204	50	268	9.97
50	230	41	191	19.59	169	33	160	16.10	165	39	207	10.66
100	185	31	139	22.56	80	14	65	20.05	40	8	42	13.53
200	76	12	53	24.91	58	10	43	22.73	14	2	11	19.97
300	46	7	30	26.79	40	6	28	24.94	15	2	11	22.79
400	91	13	56	29.19	45	7	29	27.19	15	2	10	23.83
500	157	23	92	31.23	60	9	37	29.24	16	2	11	24.59
600	195	27	110	32.34	78	11	45	30.98	17	3	11	25.35
700	184	26	102	33.03	96	14	54	32.19	22	3	14	26.08
800	154	21	84	33.44	120	17	65	33.06	25	4	16	26.74
900	134	18	72	33.89	135	18	72	33.53	32	5	20	27.42
1000	123	17	65	34.11	146	20	78	33.62	40	6	24	28.09
1100	114	15	59	34.21	153	21	81	33.48	44	6	26	28.65
1200	112	15	58	34.20	166	22	87	33.22	50	7	29	29.19
1300	110	15	56	34.18	175	24	92	32.87	55	8	31	29.66
1400	112	15	57	34.13	188	25	98	32.52	67	9	37	30.16
1500	115	15	58	34.04	199	27	104	32.17	75	10	40	30.47
2000	134	17	66	33.06	220	30	113	30.90	106	14	53	32.05
3000	152	20	73	29.64	225	30	112	28.19	NA	NA	NA	NA
4000	169	22	81	26.04	230	30	114	24.87	NA	NA	NA	NA

example stations around the world ocean and the Mediterranean (SC: Southern California (120.5° W, 29.5° N); WP: Western Pacific (126.5° E, 11.5° N); CH: Chile (75.5° W, 33.5° S); WA: Western Africa (6.5° E, 15.5° S); BB: Bay of Bengal (87.5° E, 18.5° N); MD: Mediterranean (18.5° E, 35.5° N)).

4.1 Describing the oxygen supply potential of the ocean including temperature effects: $[O_2]$ vs. SP_{O_2}

The leftmost column per station in Table 3 and Fig. 1 (both panels) show classical oxygen concentration profiles, and the second column in Table 3 and Fig. 2 show depth profiles of our newly defined oxygen supply potential SP_{O_2} (Eq. 10). It can be clearly seen that, while the general shape of the profiles is similar due to the dominating oxygen signal, there are marked differences in the overall range and especially at depth.

Those differences can be attributed to the effect of temperature-dependent diffusivity that is included in the definition of SP_{O_2} . For example, while the oxygen concentration increases again to about 60 % of surface values at 4000 m depth for the three Pacific Ocean stations shown (left panel, Fig. 1), SP_{O_2} values (left panel, Fig. 2) increase only to about 40 % of surface values due to colder temperatures limiting diffusion at depth. Similarly, the right panels of Figs. 1 and 2 show that, while the oxygen concentration at the Western Africa station rises above Mediterranean values at a depth of about 1500 m (Fig. 1), SP_{O_2} values remain higher in the Mediterranean all the way down to 4000 m depth (Fig. 2) due to diffusivity-enhancing higher temperatures. In the profiles shown for the station off Chile (CH, left panels of Figs. 1 and 2), the well-known horizontal penetration of an oxygen maximum into the oxygen minimum zone (Wyrтки, 1962) is reflected in the calculated SP_{O_2} values; however, the local maximum is less pronounced for SP_{O_2} than for $[O_2]$ due to the effect of temperature. The sample station in the Mediterranean (MD, right panels of Figs. 1 and 2), where there is a combination of the least diffusive restriction due to higher temperatures and a mean oxygen concentration being nearly twice as high as the site examined off Southern California (212 vs. 114 $\mu\text{mol kg}^{-1}$), results in the highest deep water oxygen supply potential (SP_{O_2}) values for locations we have examined. At the Bay of Bengal station (BB, right panel of Fig. 2), the waters at 800 m and below have a higher oxygen supply potential than the Southern California (SC) station, but at shallower depths the situation is reversed.

4.2 Incorporating a generic description of the influence of fluid flow velocity on dissolved gas exchange:

E_{max}

The quantity E_{max} (Eq. 12, Fig. 3, third column per station in Table 3) determines the combined influences of oxygen concentration, temperature, and fluid flow velocity over gas

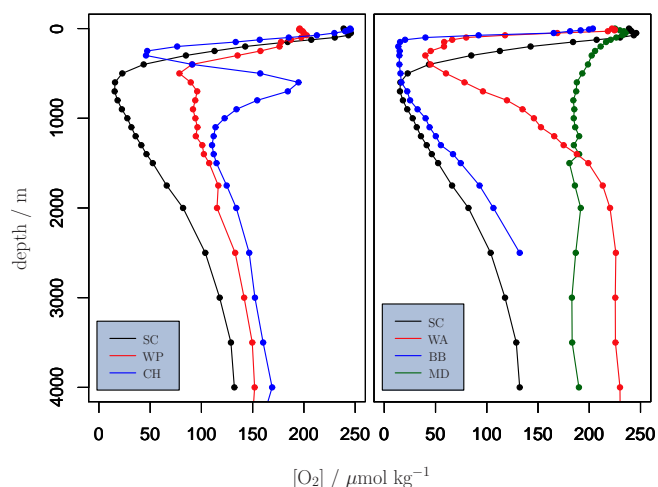


Fig. 1. $[O_2]$ depth profiles of the water column at different hydrographical stations around the world (SC: Southern California (120.5° W, 29.5° N); CH: Chile (75.5° W, 33.5° S); WP: Western Pacific (126.5° E, 11.5° N); WA: Western Africa (6.5° E, 15.5° S); MD: Mediterranean (18.5° E, 35.5° N); BB: Bay of Bengal (87.5° E, 18.5° N)).

exchange surfaces, so as to provide an estimate of the maximal diffusive transport rates per unit gas exchange area that the ocean can support. Using a canonical constant mean flow over the animal respiratory surface of $u_{100} = 2 \text{ cm s}^{-1}$ we can visualize example profiles of our quantity E_{max} at our example stations in the world oceans (Fig. 3), which are, due to the constant u_{100} , very similar in shape to the SP_{O_2} profiles in Fig. 2. To calculate E_{max} values and profiles for specific purposes, detailed flow fields and organism-specific descriptions for the DBL thickness L should be used or more specific molecular exchange models employed (see, e.g., Lazier and Mann, 1989; Karp-Boss et al., 1996). Here, we define E_{max} with a generic description of its dependency on L and thus fluid flow velocity u_{100} .

While being simplified, the description for the DBL thickness implemented here reproduces the important general non-linear dependency of L on the fluid flow velocity u_{100} , and the dependency of this relation on temperature (leftmost panel in Fig. 4). All animals require some form of fluid flow over their respiratory interfaces, and this, together with the shape of the surface, will determine the boundary layer thickness; and the relationship between external flow and boundary layer thickness will be controlled by the same physical processes. While equivalently one could plot the mass transfer coefficient K , we plot the DBL thickness L here (similar to Santschi et al., 1991), as it can be better visualized and intuitively understood. K , however, is equivalent to the “gas transfer velocity” or “piston velocity” commonly used to describe air–sea gas exchange, both for the open ocean (Wanninkhof, 1992) and coastal seas (e.g. Gypens et al., 2004) and estuaries (Hofmann et al., 2008), so the underlying simplified

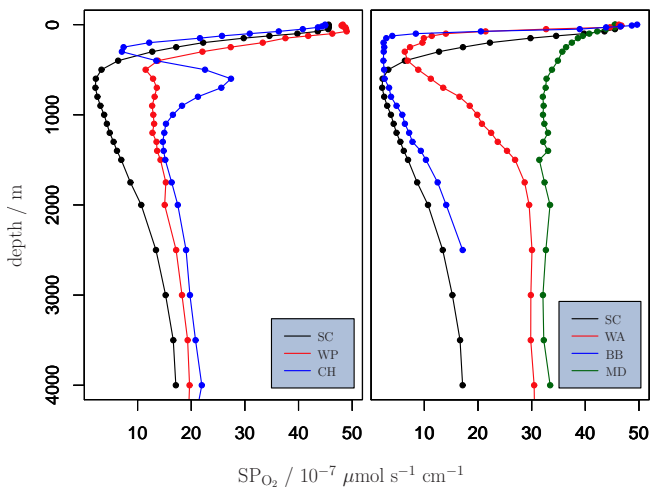


Fig. 2. Oxygen supply potential SP_{O_2} depth profiles of the water column at different hydrographical stations around the world (SC: Southern California (120.5° W, 29.5° N); CH: Chile (75.5° W, 33.5° S); WP: Western Pacific (126.5° E, 11.5° N), WA: Western Africa (6.5° E, 15.5° S), MD: Mediterranean (18.5° E, 35.5° N); BB: Bay of Bengal (87.5° E, 18.5° N)).

physical formalism is the same. The limit case of $u_{100} \rightarrow 0$ would yield $L \rightarrow \infty$. This example formulation for L as a function of u_{100} is thus not defined in a physically meaningful way for zero flow velocity and should not be used for the stagnant water case. Here we plot L with a minimum of $u_{100} = 0.5 \text{ cm s}^{-1}$, which can be seen as an operational lower limit.

4.3 Revealing the separate influences of temperature, flow, and hydrostatic pressure on gas exchange: C_f

To explicitly single out the influence of temperature and fluid flow on gas exchange, which is co-mingled with the oxygen signal in profiles of SP_{O_2} and E_{\max} , and to additionally incorporate the effect of hydrostatic pressure when comparing various oceanic regions in their ability to support given laboratory-determined respiratory rates E , we have defined the quantity C_f . C_f profiles can then be compared to $[O_2]$ profiles to determine oceanic regions that support the given oxygen demand E .

Due to the nonlinear dependency of the thickness of the diffusive boundary layer L on the current velocity u_{100} , the minimal oxygen concentration C_f supporting a given oxygen uptake rate E is also a nonlinear function of u_{100} . The middle panel of Fig. 4 explicitly visualizes this dependency for different temperatures but constant pressure and salinity, and the right panel of Fig. 4 depicts this dependency for different hydrostatic pressures. The left panel of Fig. 5 shows depth profiles of C_f for the SC example hydrographical station (i.e. with in situ temperature, salinity and pressure) for three different values for u_{100} . This further illustrates the sensitivity of C_f with respect to u_{100} .

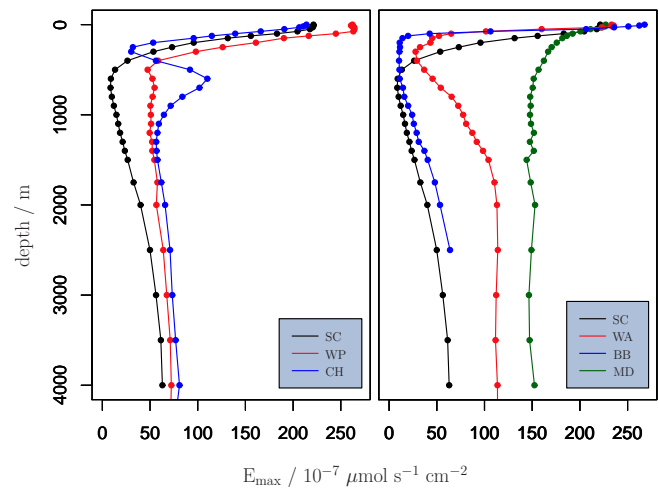


Fig. 3. Generic maximal theoretical oxygen supply rate E_{\max} depth profiles of the water column at different hydrographical stations around the world (SC: Southern California (120.5° W, 29.5° N); CH: Chile (75.5° W, 33.5° S); WP: Western Pacific (126.5° E, 11.5° N), WA: Western Africa (6.5° E, 15.5° S), MD: Mediterranean (18.5° E, 35.5° N); BB: Bay of Bengal (87.5° E, 18.5° N)). A generic flow velocity of $u_{100} = 2 \text{ cm s}^{-1}$ is assumed for all depths to calculate L . If available, detailed flow profiles can be used here, as well as organism-specific descriptions for L .

It can be shown for the range of u_{100} values in the middle panel of Fig. 4, that a u_{100} decrease by half results in approximately a doubling of C_f (i.e. C_f is roughly proportional to the inverse of u_{100}). The nonlinear character of the relation between the fluid flow velocity u_{100} and the limit for free stream oxygen concentration C_f is such that there is a low dependency when $u_{100} > 2 \text{ cm s}^{-1}$ and very high dependency when $u_{100} < 1 \text{ cm s}^{-1}$. This is a result of the respective behavior of the thickness of the diffusive boundary layer L on u_{100} , as also described by, e.g., Garmo et al. (2006).

The right panel of Fig. 5 shows example depth profiles of C_f at the SC station for three different respiratory rates E , on realistic orders of magnitude, to express the sensitivity of C_f with respect to E .

The general shape of C_f depth profiles in Fig. 5 can be explained by comparison of C_f (Eq. 15) with its direct predecessor quantity p_f (Eq. 14), the minimal oxygen partial pressure required to support E . The quantity C_f directly includes effects of diffusivity, boundary layer thickness, and temperature and hydrostatic pressure effects on partial pressure. The predecessor quantity p_f expresses only effects on diffusivity and boundary layer thickness. As temperature decreases with depth, so does the “efficiency” of diffusion, with the result that L increases. This translates into a higher p_f with depth, i.e. a higher necessary pO_2 to sustain the given oxygen consumption rate E . The limit for oxygen concentration C_f initially follows suit, but as hydrostatic pressure increases with depth, so does the pO_2 for a given $[O_2]$ (Enns et al., 1965).

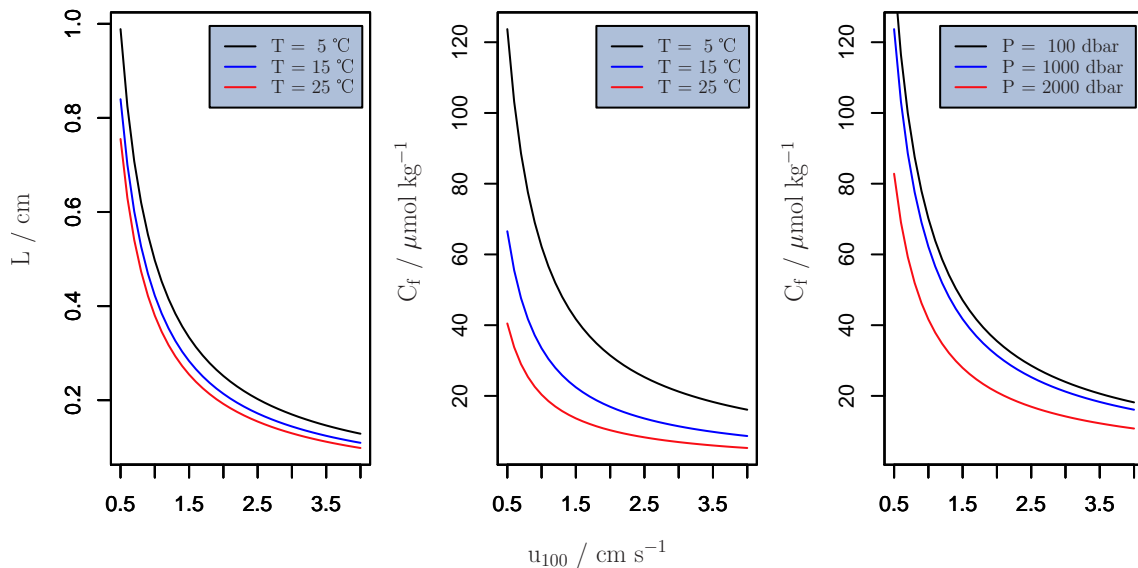


Fig. 4. The influence of flow velocity u_{100} , temperature T and hydrostatic pressure P on the DBL thickness L and C_f , the minimal oxygen concentration supporting a given laboratory-determined oxygen uptake rate E . The dependency of L (and all derived quantities) on u_{100} is based on the simple exemplary model description employed here. While individual organism-specific dependencies may vary in detail, the general dependency of L on the flow velocity is captured here. For all calculations we assume a generic constant value of $E = 20 \times 10^{-7} \mu\text{mol s}^{-1} \text{cm}^{-2}$. Unless stated otherwise in the legend, latitude = 29.5°N , $S = 34$, $T = 5^\circ\text{C}$, $P = 100 \text{bar}$, $E = 20 \times 10^{-7} \mu\text{mol s}^{-1} \text{cm}^{-2}$, $T_E = 5^\circ\text{C}$, and $S_E = 34$.

This means that p_f , the $p\text{O}_2$ necessary to sustain E , which is more or less constant with depth from below 2000 m as temperature does not change anymore, is sustained by a smaller and smaller oxygen concentration: C_f decreases from about 2000 m on.

Different ocean basins exhibit markedly different temperature and salinity profiles; these differences affect the quantity C_f since this subsumes the influences of temperature, salinity and hydrostatic pressure on diffusive gas transport. Figure 6 and the fourth column in Table 3 show C_f depth profiles for our example hydrographical stations, assuming a constant current velocity of 2cm s^{-1} . In the Pacific, the profiles are rather similar, while warm enclosed seas like the Mediterranean differ markedly. Here, due to warm temperatures throughout the water column, the entire profiles are shifted towards lower C_f values. It is remarkable that in the Mediterranean, the oxygen concentration at 4000 m depth required to sustain a given oxygen consumption rate is lower than at the surface. In the Atlantic the C_f maximum is sharply defined at around 1000 m depth; in the Pacific the maximum is more broadly defined at around the same depth, in keeping with classical hydrographic profiles. In the Indian Ocean (Bay of Bengal), the C_f maximum is deeper at $\approx 2000 \text{m}$. Given the marked similarity of C_f profiles in the Pacific (left panel of Fig. 6), one can conclude that the differences in oxygen supply potential SP_{O_2} between various stations in the Pacific (left panel of Fig. 2) are mainly due to differences in oxygen concentration profiles. This is not the case for the example stations that are not located in the Pacific (right pan-

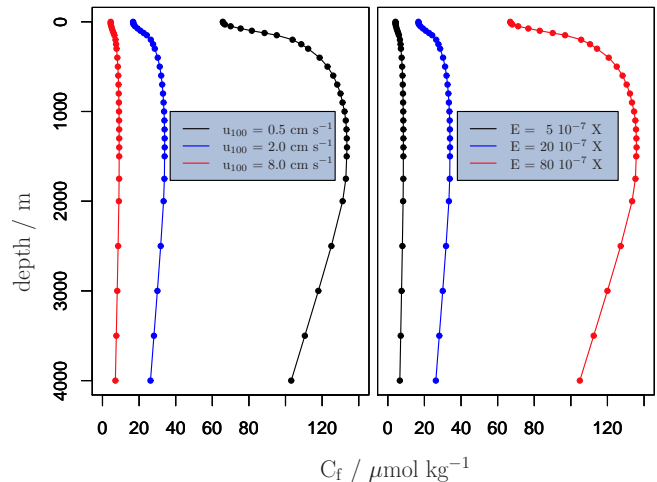


Fig. 5. The influence of flow velocity u_{100} and examples of given laboratory-determined oxygen uptake rates E ($X = \mu\text{mol s}^{-1} \text{cm}^{-2}$), along depth profiles of temperature T , and hydrostatic pressure P at the Pacific station SC off Southern California (120.5°W , 29.5°N). $T_E = 5^\circ\text{C}$, and $S_E = 34$.

els of Figs. 2 and 6), where the effects of temperature and pressure considerably contribute to the differences in SP_{O_2} profiles.

Even though our particular description of the dependency is generalized, the fact that the limit for oxygen concentration C_f is dependent on current velocity makes it necessary

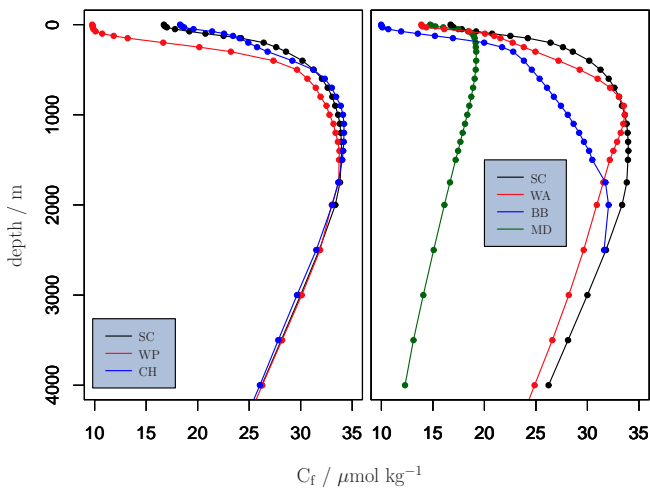


Fig. 6. Minimal oxygen concentration C_f , supporting a given laboratory-determined oxygen uptake rate, depth profiles of the water column at different hydrographical stations around the world (SC: Southern California (120.5° W, 29.5° N); CH: Chile (75.5° W, 33.5° S); WP: Western Pacific (126.5° E, 11.5° N), WA: Western Africa (6.5° E, 15.5° S), MD: Mediterranean (18.5° E, 35.5° N); BB: Bay of Bengal (87.5° E, 18.5° N)). A generic flow velocity of $u_{100} = 2 \text{ cm s}^{-1}$ is assumed for all depths to calculate L . If available, detailed flow profiles can be used here, as well as organism-specific descriptions for L . For all calculations we assume a generic constant value of $E = 20 \times 10^{-7} \text{ } \mu\text{mol s}^{-1} \text{ cm}^{-2}$

that water flow rates be included in the set of variables that are controlled or reported when comparing different systems or different animal responses (e.g. Stachowitsch et al., 2007; Riedel et al., 2008; Haselmair et al., 2010).

5 Summary and conclusions

In this publication we define new quantities that describe the ocean's ability to supply oxygen, based on diffusive boundary transport rate limitations. These quantities subsume well-known oceanic physical properties relevant to diffusive boundary transport into functions that may be used for various purposes, including estimating the impacts of ocean warming and declines in dissolved O_2 .

The oxygen supply potential SP_{O_2} and the maximal oxygen supply rate E_{max} that an environment can sustain are the more general parameters that could be used to map specific oceanic regions according to their ability to supply oxygen. The limit for oxygen concentration C_f supporting a given demand rate E is the quantity that explicitly expresses the effects of temperature, flow and hydrostatic pressure, without the visual obstruction by the dominant oxygen concentration signal. C_f values can be used to approximate the hospitability of certain regions for particular animals with known oxygen uptake rate requirements.

All our newly defined quantities express the requirements and limitations imposed only by the oceanic physical environment. The results from example oceanographic stations around the world strongly suggest a greater diversity of regions and a more complex response of biogeochemical cycles to ocean warming than anticipated from the simple change in O_2 concentration alone. It should not be surprising that the fields produced appear superficially to resemble traditional O_2 concentration profiles and maps; descriptions of the formation of the $[\text{O}_2]$ minimum and well-established gradients along major ocean circulation pathways are dominant features and powerful drivers that have long been described (Wyrski, 1962). It is for this reason that the relatively crude representation of various limits by simple concentration values has been in use for so long; they are familiar and have served as reasonable approximations. But the basic kinetic rate representation given here allows for much greater insight, in particular for different oceanic depth realms and for an ocean changing simultaneously in T and $[\text{O}_2]$. For example the basic solubility equation always results in lower O_2 concentration from ocean warming, which may be interpreted as more limiting to aerobic life. But when combined with the essential temperature and pressure dependencies of $p\text{O}_2$ and diffusivity, a more complex picture emerges.

Acknowledgements. This work was supported by a grant to the Monterey Bay Aquarium Research Institute from the David & Lucile Packard Foundation.

Edited by: F. Meysman

References

- Biron, P. M., Robson, C., Lapointe, M. F., and Gaskin, S. J.: Comparing different methods of bed shear stress estimates in simple and complex flow fields, *Earth Surf. Proc. Landf.*, 29, 1403–1415, doi:10.1002/esp.1111, 2004.
- Boudreau, B. P.: *Diagenetic Models and Their Implementation*, Springer, Berlin, 1996.
- Bryden, H. L.: New polynomials for thermal expansion, adiabatic temperature gradient and potential temperature of sea water, *Deep-Sea Res.*, 20, 401–408, 1973.
- Chen, C. T. A., Bychkov, A. S., Wang, S. L., and Pavlova, G. Y.: An anoxic Sea of Japan by the year 2200?, *Mar. Chem.*, 67, 249–265, 1999.
- Childress, J. J. and Seibel, B. A.: Life at stable low oxygen levels: Adaptations of animals to oceanic oxygen minimum layers, *J. Exp. Biol.*, 201, 1223–1232, 1998.
- Enns, T., Scholander, P. F., and Bradstreet, E. D.: Effect of Hydrostatic Pressure on Gases Dissolved in Water, *J. Phys. Chem.*, 69, 389–391, 1965.
- Feder, M. E. and Burggren, W. W.: Cutaneous gas exchange in vertebrates: design, patterns, control and implications, *Biol. Rev. Camb. Philos. Soc.*, 60, 1–45, 1985.

- Fofonoff, N. P.: Computation of potential temperature of seawater for an arbitrary reference pressure, *Deep-Sea Res.*, 24, 489–491, 1977.
- Fofonoff, N. P. and Millard, R. C. J.: Algorithms for computation of fundamental properties of seawater, UNESCO technical papers in marine science, 44, 55 pp., 1983.
- Garcia, H. E. and Gordon, L. I.: Oxygen Solubility in Seawater – Better Fitting Equations, *Limnol. Oceanogr.*, 37, 1307–1312, 1992.
- Garcia, H. E., Locarnini, R. A., Boyer, T. P., Antonov, J. I., Baranova, O. K., Zweng, M. M., and Johnson, D. R.: World Ocean Atlas 2009, in: Volume 3: Dissolved Oxygen, Apparent Oxygen Utilization, and Oxygen Saturation, edited by: Levitus, S., NOAA Atlas NESDIS 70, US Government Printing Office, Washington DC, 344 pp., 2010.
- Garmo, O., Naqvi, K., Royset, O., and Steinnes, E.: Estimation of diffusive boundary layer thickness in studies involving diffusive gradients in thin films (DGT), *Anal. Bioanal. Chem.*, 386, 2233–2237, doi:10.1007/s00216-006-0885-4, 2006.
- Gypens, N., Lancelot, C., and Borges, A. V.: Carbon dynamics and CO₂ air-sea exchanges in the eutrophied coastal waters of the Southern Bight of the North Sea: a modelling study, *Biogeosciences*, 1, 147–157, doi:10.5194/bg-1-147-2004, 2004.
- Haselmair, A., Stachowitsch, M., Zuschin, M., and Riedel, B.: Behaviour and mortality of benthic crustaceans in response to experimentally induced hypoxia and anoxia in situ, *Mar. Ecol.-Prog. Ser.*, 414, 195–208, 2010.
- Helm, K. P., Bindoff, N. L., and Church, J. A.: Observed decreases in oxygen content of the global ocean, *Geophys. Res. Lett.*, 38, L23602, doi:10.1029/2011GL049513, 2011.
- Hickey, B., Baker, E., and Kachel, N.: Suspended particle movement in and around Quinault submarine canyon, *Mar. Geol.*, 71, 35–83, doi:10.1016/0025-3227(86)90032-0, 1986.
- Hofmann, A. F., Soetaert, K., and Middelburg, J. J.: Present nitrogen and carbon dynamics in the Scheldt estuary using a novel 1-D model, *Biogeosciences*, 5, 981–1006, doi:10.5194/bg-5-981-2008, 2008.
- Hofmann, A. F., Soetaert, K., Middelburg, J. J., and Meysman, F. J. R.: AquaEnv: An Aquatic Acid-Base Modelling Environment in R, *Aquat. Geochem.*, 16, 507–546, 2010.
- Hofmann, A. F., Peltzer, E. T., Walz, P. M., and Brewer, P. G.: Hypoxia by degrees: Establishing definitions for a changing ocean, *Deep-Sea Res. Pt. I*, 58, 1212–1226, doi:10.1016/j.dsr.2011.09.004, 2011.
- Hofmann, A. F., Peltzer, E. T., and Brewer, P. G.: Kinetic bottlenecks to chemical exchange rates for deep-sea animals – Part 2: Carbon Dioxide, *Biogeosciences*, 10, 2409–2425, doi:10.5194/bg-10-2409-2013, 2013.
- Hughes, G. M.: The dimensions of fish gills in relation to their function, *J. Exp. Biol.*, 45, 177–195, 1966.
- Jenkins, W. J.: The biogeochemical consequences of changing ventilation in the Japan/East Sea, *Mar. Chem.*, 108, 137–147, doi:10.1016/j.marchem.2007.11.003, 2008.
- Karp-Boss, L., Boss, E., and Jumars, P.: Nutrient fluxes to planktonic osmotrophs in the presence of fluid motion, *Oceanogr. Mar. Biol.*, 34, 71–107, 1996.
- Lazier, J. R. N. and Mann, K. H.: Turbulence and diffusive layers around small organisms, *Deep-Sea Res.*, 36, 1721–1733, 1989.
- Levitus, S., Antonov, J., and Boyer, T. P.: Warming of the world ocean, *Geophys. Res. Lett.*, 32, 1955–2003, 2005.
- Lyman, J. M., Good, S. A., Gouretski, V. V., Ishii, M., Johnson, G. C., Palmer, M. D., Smith, D. M., and Willis, J. K.: Robust warming of the global upper ocean, *Nature*, 465, 334–337, 2010.
- Maxime, V., Peyraud-Waitzenegger, M., Claireaux, G., and Peyraud, C.: Effects of rapid transfer from sea water to fresh water on respiratory variables, blood acid-base status and O₂ affinity of haemoglobin in Atlantic salmon (*Salmo salar* L.), *J. Comp. Physiol. B*, 160, 31–39, 1990.
- Millero, F. J. and Poisson, A.: International One-Atmosphere Equation of State of Seawater, *Deep-Sea Res.*, 28, 625–629, 1981.
- Palumbi, S. R., Sandifer, P. A., Allan, J. D., Beck, M. W., Fautin, D. G., Fogarty, M. J., Halpern, B. S., Incze, L. S., Leong, J.-A., Norse, E., Stachowicz, J. J., and Wall, D. H.: Managing for ocean biodiversity to sustain marine ecosystem services, *Front. Ecol. Environ.*, 7, 204–211, doi:10.1890/070135, 2009.
- Pelster, B. and Burggren, W. W.: Disruption of Hemoglobin Oxygen Transport Does Not Impact Oxygen-Dependent Physiological Processes in Developing Embryos of Zebra Fish (*Danio rerio*), *Circ. Res.*, 79, 358–362, 1996.
- Piiper, J.: Respiratory gas exchange at lungs, gills and tissues: mechanisms and adjustments, *J. Exp. Biol.*, 100, 5–22, 1982.
- Pinczewski, W. V. and Sideman, S.: A model for mass (heat) transfer in turbulent tube flow. Moderate and high Schmidt (Prandtl) numbers, *Chem. Eng. Sci.*, 29, 1969–1976, doi:10.1016/0009-2509(74)85016-5, 1974.
- Pinder, A. W. and Burggren, W. W.: Ventilation and partitioning of oxygen uptake in the frog *Rana pipiens*: effects of hypoxia and activity, *J. Exp. Biol.*, 126, 453–468, 1986.
- Pinder, A. W. and Feder, M. E.: Effect of Boundary Layers on Cutaneous Gas Exchange, *J. Exp. Biol.*, 154, 67–80, 1990.
- Poertner, H. O. and Knust, R.: Climate Change Affects Marine Fishes Through the Oxygen Limitation of Thermal Tolerance, *Science*, 315, 95–97, doi:10.1126/science.1135471, 2007.
- R Development Core Team: R: A Language and Environment for Statistical Computing, R Foundation for Statistical Computing, Vienna, Austria, <http://www.R-project.org>, ISBN 3-900051-07-0, 2010.
- Riedel, B., Zuschin, M., Haselmair, A., and Stachowitsch, M.: Oxygen depletion under glass: Behavioural responses of benthic macrofauna to induced anoxia in the Northern Adriatic, *J. Exp. Mar. Biol. Ecol.*, 367, 17–27, doi:10.1016/j.jembe.2008.08.007, 2008.
- Santschi, P. H., Anderson, R. F., Fleisher, M. Q., and Bowles, W.: Measurements of Diffusive Sublayer Thicknesses in the Ocean by Alabaster Dissolution, and Their Implications for the Measurements of Benthic Fluxes, *J. Geophys. Res.*, 96, 10641–10657, doi:10.1029/91JC00488, 1991.
- Schlitzer, R.: Ocean Data View 4, <http://odv.awi.de/>, 2010.
- Seibel, B. A., Chausson, F., Lallier, F. H., Zal, F., and Childress, J. J.: Vampire blood: respiratory physiology of the vampire squid (Cephalopoda: Vampyromorpha) in relation to the oxygen minimum layer, *Exp. Biol. Online*, 4, 1–10, doi:10.1007/s00898-999-0001-2, 1999.

- Shaw, D. A. and Hanratty, T. J.: Turbulent mass transfer rates to a wall for large Schmidt numbers, *AIChE J.*, 23, 28–37, doi:10.1002/aic.690230106, 1977.
- Soetaert, K., Petzoldt, T., and Meysman, F.: marelac: Tools for Aquatic Sciences, <http://CRAN.R-project.org/package=marelac>, r package version 2.1, 2010.
- Stachowitsch, M., Riedel, B., Zuschin, M., and Machan, R.: Oxygen depletion and benthic mortalities: the first in situ experimental approach to documenting an elusive phenomenon, *Limnol. Oceanogr.-Methods*, 5, 344–352, 2007.
- Sternberg, R. W.: Friction factors in tidal channels with differing bed roughness, *Mar. Geol.*, 6, 243–260, doi:10.1016/0025-3227(68)90033-9, 1968.
- Stolper, D. A., Revsbech, N. P., and Canfield, D. E.: Aerobic growth at nanomolar oxygen concentrations, *P. Natl. Acad. Sci. USA*, 107, 18755–18760, 2010.
- Stramma, L., Johnson, G. C., Sprintall, J., and Mohrholz, V.: Expanding oxygen-minimum zones in the tropical oceans, *Science*, 320, 655–658, 2008.
- Tallis, H., Lester, S. E., Ruckelshaus, M., Plummer, M., McLeod, K., Guerry, A., Andelman, S., Caldwell, M. R., Conte, M., Copps, S., Fox, D., Fujita, R., Gaines, S. D., Gelfenbaum, G., Gold, B., Kareiva, P., Kim, C., Lee, K., Papenfus, M., Redman, S., Silliman, B., Wainger, L., and White, C.: New metrics for managing and sustaining the ocean's bounty, *Mar. Policy*, 36, 303–306, doi:10.1016/j.marpol.2011.03.013, 2011.
- Wanninkhof, R.: Relationship between Wind-Speed and Gas-Exchange over the Ocean, *J. Geophys. Res.-Oceans*, 97, 7373–7382, 1992.
- Weiss, R. F.: Solubility of Nitrogen, Oxygen and Argon in Water and Seawater, *Deep-Sea Res.*, 17, 721–735, 1970.
- Weiss, R. F.: Carbon dioxide in water and seawater: the solubility of a non-ideal gas, *Mar. Chem.*, 2, 203–215, 1974.
- Wood, P. E. and Petty, C. A.: New model for turbulent mass transfer near a rigid interface, *AIChE J.*, 29, 164–167, doi:10.1002/aic.690290126, 1983.
- Wyrski, K.: The oxygen minima in relation to ocean circulation, *Deep-Sea Res.*, 9, 11–23, 1962.
- Zeebe, R. E. and Wolf-Gladrow, D.: CO₂ in Seawater: Equilibrium, Kinetics, Isotopes, no. 65 in Elsevier Oceanography Series, Elsevier, 1st Edn., 2001.